The Elusive Dimethylhydroxysulfuranyl Radical. An Intermediate or a Transition State?

Ming Gu and Frantisek Turecek*

Contribution from the Department of Chemistry, BG-10, University of Washington, Seattle, Washington 98195. *Received January 30, 1992*

Abstract: The stability and dissociations of dimethylhydroxysulfuranyl radical, a key intermediate in the atmospheric oxidation of dimethyl sulfide, have been investigated by neutralization-reionization mass spectrometry and ab initio calculations. Dimethylhydroxysulfuranyl radical (**1**) and its d_6 derivative **2** were generated in the gas phase by neutralization of protonated dimethylsulfoxide and dimethylsulfoxide-d_6, respectively. Hypervalent radical **1** dissociates completely within 4.5 μs to CH_3SOH by loss of $CH_3^\bullet$ and to $(CH_3)_2S$ by loss of $OH^\bullet$. These primary products undergo further extensive dissociations. **2** also shows a minor dissociation to $(CD_3)_2SO$ by loss of hydrogen atom in addition to the formation of CD_3SOH and $(CD_3)_2S$ by losses of $CD_3^\bullet$ and $OH^\bullet$, respectively. Ab initio calculations (MP4/6-31G*) find no potential energy minimum for **1** that collapses without barrier by oxygen-sulfur or carbon-sulfur bond fissions. Vertical neutralization of ion 1^+ produces an unstable radical **1** lying 193 kJ mol^{-1} above the lowest energy $(CH_3)_2S$ and $OH^\bullet$ products. Relative energies of all primary dissociation products were calculated and compared with experimental data.

Dimethyl sulfide (DMS), a major natural pollutant produced by biomass decay and emitted by oceans, undergoes complex photochemical oxidation in the atmosphere to produce sulfur dioxide, methanesulfonic acid, and dimethyl sulfone.[1] The diurnal atmospheric chemistry of DMS is believed to commence with the gas-phase reaction with hydroxyl radical generated photochemically (eq 1).[2] The main reaction channel in eq 1 is hydrogen

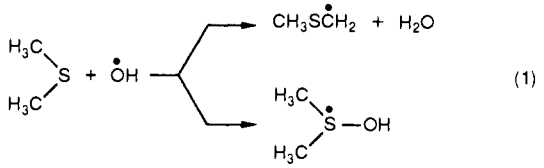

(1)

1

atom abstraction forming water and methylthiomethyl radical. As a side reaction, attack of the hydroxyl radical at the DMS sulfur atom gives rise to the dimethylhydroxysulfuranyl radical (**1**) that dissociates rapidly to products, presumably methanesulfenic acid and methyl radical.[2] The existence of **1** as a reactive intermediate rather than a transition state has been inferred from kinetic analysis of the DMS reaction with $OH^\bullet$ generated by laser photolysis.[3] However, no direct spectroscopic observation of **1** as a reactive intermediate has been reported, although it was asssumed that **1** exists as a thermalized, steady-state intermediate with a half-life of ca. 2×10^{-7} s.[3,4]

Structure **1** represents a hypervalent sulfur radical belonging to a class of highly unstable species of considerable recent theoretical[5] and experimental interest.[6] Hypervalent radicals as a rule exist in very shallow potential energy minima (if any at all) and dissociate rapidly by simple bond cleavage.[7] This behavior somewhat contrasts the stability estimates of **1** for which a substantial binding energy has been estimated (54 kJ mol^{-1}).[3]

The question of whether **1** is an intermediate or a transition state has implications for both the intrinsic stability of this hypervalent species and, more importantly, the kinetics of the DMS-$OH^\bullet$ reaction. If **1** is an intermediate, its dissociation kinetics and product branching ratios will be governed by the critical energies of the competing unimolecular dissociations, e.g., eqs 2-4. By contrast, if **1** is a transition state, there should be

$$\mathbf{1} \rightarrow CH_3SCH_3 + OH^\bullet \quad (2)$$

$$\mathbf{1} \rightarrow CH_3SOH + CH_3^\bullet \quad (3)$$

$$\mathbf{1} \rightarrow (CH_3)_2SO + H^\bullet \quad (4)$$

a single reaction path connecting DMS and $OH^\bullet$ with products, as no branching can occur in the transition state due to the Murrell-Laidler rules.[8] Formation of other products then should proceed through different transition states or intermediates. Direct evidence for the existence of **1** is therefore essential for the understanding of the dimethyl sulfide oxidation kinetics.

In this work we generate **1** directly by gas-phase electron-transfer neutralization of the corresponding cation, $(CH_3)_2S^+OH$, and analyze the products by mass spectrometry. This neutralization-reionization mass spectrometric technique (NRMS)[7a,9] has

(1) (a) Lovelock, J. E.; Maggs, R. J.; Rasmussen, R. A. *Nature (London)* **1972**, *37*, 452. (b) Andreae, M. O.; Ferek, R. J.; Bermond, F.; Byrd, K. P.; Engstrom, R. T.; Hardin, S.; Houmere, P. D.; LeMarrec, F.; Raemdonck, H.; Chatfield, R. B. *J. Geophys. Res., [Atmos.]* **1985**, *90*, 12891. (c) For reviews, see: Saltzman, E. S., Cooper, W. J., Eds. *Biogenic Sulfur in the Environment*; American Chemical Society: Washington, DC, 1989. (d) Graedel, T. E. *Rev. Geophys. Space Phys.* **1977**, *15*, 421-428.

(2) (a) Atkinson, R.; Perry, R. A.; Pitts, J. N., Jr. *Chem. Phys. Lett.* **1978**, *54*, 14. (b) For a review, see: Plane, J. M. C. In *Biogenic Sulfur in the Environment*; Saltzman, E. S., Cooper, W. J., Eds.; American Chemical Society: Washington, DC, 1989; Chapter 24, p 404-422.

(3) Hynes, A. J.; Wine, P. H.; Semmes, D. H. *J. Phys. Chem.* **1986**, *90*, 4148-4156.

(4) Hynes, A. J.; Wine, P. H. in ref 1c, Chapter 25, p 424-435.

(5) (a) Kassab, E.; Evleth, E. M. *J. Am. Chem. Soc.* **1987**, *109*, 1653-1661. (b) Demolliens, A.; Eisenstein, O.; Hiberty, P. C.; Lefour, J. M.; Ohanessian, G.; Shaik, S. S.; Volatron, F. *J. Am. Chem. Soc.* **1989**, *111*, 5623-5631. (c) Reed, A. E.; Schleyer, P. v. R. *J. Am. Chem. Soc.* **1990**, *112*, 1434-1445.

(6) (a) Perkins, C. W.; Martin, J. C.; Arduengo, A. J.; Lau, W.; Alegria, A.; Kochi, J. K. *J. Am. Chem. Soc.* **1980**, *102*, 7753-7759. (b) Perkins, C. W.; Clarkson, R. B.; Martin, J. C. *J. Am. Chem. Soc.* **1986**, *108*, 3206-3210. (c) Perkins, C. W.; Martin, J. C. *J. Am. Chem. Soc.* **1986**, *108*, 3211-3214. (d) Martin, J. C.; Perozzi, E. F. *Science (Washington, D.C.)* **1976**, *191*, 154-159. (e) Martin, J. C. *Science (Washington, D.C.)* **1983**, *221*, 509-514. (f) Franz, J. A.; Roberts, D. H.; Ferris, K. F. *J. Org. Chem.* **1987**, *52*, 2256-2262. (g) Saeva, F. D.; Morgan, P. *J. Am. Chem. Soc.* **1984**, *106*, 4121-4125. (h) Anklam, E.; Margaretha, P. *Res. Chem. Intermed.* **1989**, *11*, 127-155.

(7) (a) Gellene, G. I.; Porter, R. F. *Acc. Chem. Res.* **1983**, *16*, 200-207. (b) Gellene, G. I.; Porter, R. F. *J. Chem. Phys.* **1984**, *81*, 5570-5576. (c) Gellene, G. I.; Porter, R. F. *Int. J. Mass Spectrom. Ion Processes* **1985**, *64*, 55-66. (d) Raksit, A. B.; Porter, R. F. *J. Chem. Soc., Chem. Commun.* **1987**, 500-501. (e) Raksit, A. B.; Porter, R. F. *Org. Mass Spectrom.* **1987**, *22*, 420-417. (f) Holmes, J. L.; Sirois, M. *Org. Mass Spectrom.* **1990**, *25*, 481-482.

(8) Murrell, J. N.; Laidler, K. J. *Trans. Faraday Soc.* **1968**, *64*, 371-377.

(9) (a) Danis, P. O.; Wesdemiotis, C.; McLafferty, F. W. *J. Am. Chem. Soc.* **1983**, *105*, 7454-7456. (b) Burgers, P. C.; Holmes, J. L.; Mommers, A. A.; Terlouw, J. K. *Chem. Phys. Lett.* **1983**, *102* 1-3. (c) For reviews see: Wesdemiotis, C.; McLafferty, F. W. *Chem. Rev.* **1987**, *87*, 485-500. (d) Terlouw, J. K.; Schwarz, H. *Angew. Chem., Int. Ed. Engl.* **1987**, *26*, 805-815. (e) Holmes, J. L. *Mass Spectrom. Rev.* **1989**, *8*, 513-539. (f) McLafferty, F. W. *Science (Washington, D.C.)* **1990**, *247*, 925-929.

0002-7863/92/1514-7146$03.00/0

been utilized for the generation of a number of gaseous transient species, namely, hypervalent radicals,[6] ylides and carbenes,[10] sulfenic acids and organosulfur radicals,[11] biradicals,[12] etc. In NRMS a mass-selected precursor ion of a keV kinetic energy is allowed to undergo electron transfer with atoms or molecules of thermal gas. For $(CH_3)_2S^+OH$, m/z 79, with 8 keV of kinetic energy colliding with a xenon atom, the time of interaction is $\tau \leq 10^{-14}$ s, allowing essentially vertical transition from the ion potential energy surface to that of the neutral species. This can lead to internal energy deposition in the latter due to unfavorable Franck–Condon factors.[9e,13] Unimolecular dissociations of hypervalent species, e.g., oxonium radicals,[7d-f] show peculiar branching ratios in that reactions of widely different exothermicities (up to 1 eV) are competitive, and their products can be observed simultaneously. Also, unusually large deuterium isotope effects have been reported in dissociations of several hypervalent radicals.[7]

In this work we examine the formation and unimolecular and collisionally activated dissociations of **1**, $(CD_3)_2SOH$ (**2**), and their potential fragmentation products, $CH_3SO^•$, $(CH_3)_2SO$, $CD_3SO^•$, $(CD_3)_2SO$, and $(CH_3)_2S$. To complement experimental data, the energetics of the principal dissociations are assessed by ab initio theoretical calculations.

Experimental Section

Measurements were carried out with a tandem quadrupole acceleration–deceleration mass spectrometer specially designed for neutralization–reionization studies.[14] Briefly, the instrument consists of a combined electron-impact/chemical-ionization ion source and an Extrel quadrupole analyzer as MS-I. Mass-selected or filtered ions of 50–60 eV kinetic energy are accelerated to 8 keV and transported to a collision cell (cell-I) floated at −8 kV where they are allowed to collide with a neutralization gas (Xe) at 70% ion beam transmittance (T). This corresponds to 2×10^{-5} Torr of Xe as measured outside cell-I. The remaining ions are reflected back by an ion conduit maintained at +250 V, whereas fast neutrals continue to the reionization cell (cell-II) located 60 cm downbeam. The neutrals are reionized by collisions with oxygen at 70% transmittance ($2–4 \times 10^{-5}$ Torr of O_2 as measured outside cell-II), and the ions formed are decelerated to the original kinetic energy (50–60 eV) by an electrostatic lens. The reionization cell is floated at the deceleration voltage which is scanned from 0 to −8 kV to pass positively charged ions formed from neutral fragments of variable mass and kinetic energy. High-energy ions are filtered out by an electrostatic lens, and the remaining ions are mass-analyzed by a second quadrupole mass spectrometer (Extrel) as MS-II. The latter is scanned in link with the deceleration voltage to allow passage of ions of selected mass and kinetic energy. The mass filter bandwidth was set to <0.4 amu (full width at half-maximum, fwhm) allowing unit mass resolution (<10% valley). The ion source, MS-I, collision cells, and MS-II are differentially pumped. Further, collisionally activated neutral dissociations can be monitored by admitting helium in the differentially pumped and floated conduit between cell-I and cell-II. Only neutral products are thus selected, as any ions formed by collisional reionization in this region retain their high kinetic energy and do not pass the energy filter lens.

$(CH_3)_2S^+OH$ (1^+) and $(CD_3)_2S^+OH$ (2^+) were prepared by isobutane chemical ionization of dimethyl sulfoxide (DMSO) and dimethyl sulfoxide-d_6 (DMSO-d_6, both Aldrich), respectively. Ion source conditions were as follows: temperature 185 °C, emission current 1 mA, electron energy 100 eV, isobutane pressure 3×10^{-4} Torr as measured at the ion source diffusion pump intake. In order to increase sensitivity, MS-I was operated in the rf-only mode[15] allowing passage of ions of $m/z > 17$. This results in a few artifact peaks in the NRMS spectra at m/z 25–28 and 36–43 due to neutralization of C_2H_n and C_3H_n ions from isobutane plasma within the acceleration lens. However, these fragments do not interfere with those from **1** and **2** neutral dissociations. Likewise, collisional reionization of O_2 outside cell-II gives rise to a weak to moderate peak at m/z 32 in the NR mass spectrum that overlaps with the peak of $S^{•+}$. The reported NR and NCR mass spectra are averages of 20–40 repetitive scans acquired with a home-built PC-based data system.[16]

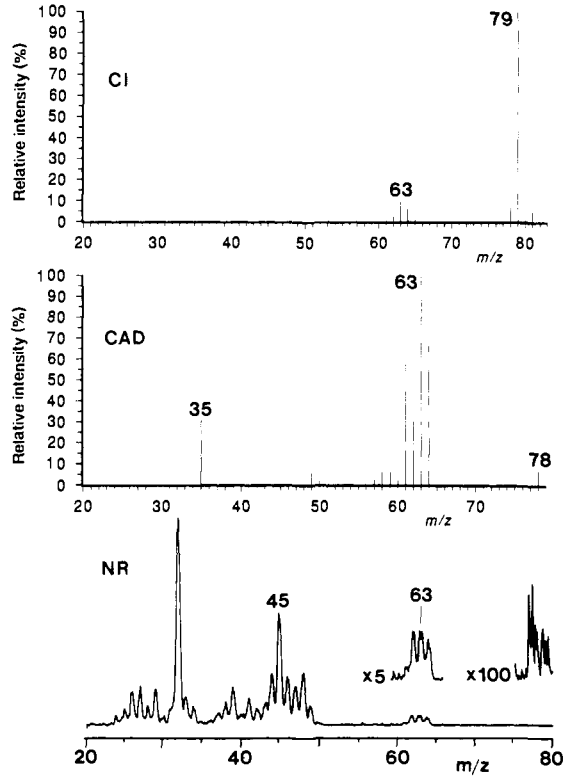

Figure 1. Top, isobutane chemical ionization mass spectrum of $(CH_3)_2SO$; middle, collisionally activated dissociation (O_2, 70% transmittance) mass spectrum of 1^+; bottom, neutralization–reionization (Xe/O_2, 70%/70% transmittance) mass spectrum of 1^+.

Collisionally activated dissociation (CAD) mass spectra were measured on a VG 7070-EQ instrument with oxygen as collision gas at 70% transmittance of the precursor ion beam at 8 keV. Product ions formed in the first field free region were monitored by scanning the electrostatic and magnet analyzers while keeping the field intensities at a constant ratio (B/E linked scan).

Calculations

Standard ab initio molecular orbital calculations[17] were carried out using the GAUSSIAN 88 program.[18] Geometry optimizations were performed with the 3-21G and 6-31G* basis sets. UHF wave functions were used for all odd-electron species. Harmonic vibrational frequencies, also calculated with the 3-21G and 6-31G* basis sets, were used both to characterize stationary points on the surface as minima (all frequencies real, representing equilibrium structures) and (after scaling by 0.9) to calculate zero-point vibrational contributions to relative energies. Improved relative energies were obtained through calculations on the HF/6-31G* optimized geometries using Møller–Plesset perturbation theory (frozen core) terminated at second (MP2), third (MP3), and fourth (MP4) orders. The MP4(SDTQ)/6-31G* electronic energies, corrected for zero-point vibrational energies, were used to

(10) (a) Sulzle, D.; Drewello, T.; van Baar, B. L. M.; Schwarz, D. *J. Am. Chem. Soc.* **1988**, *110*, 8330–8333. (b) Wesdemiotis, C.; Leyh, B.; Fura, A.; McLafferty, F. W. *J. Am. Chem. Soc.* **1990**, *112*, 8655–8660. (c) Hudgins, D. M.; Weber, A. L.; Porter, R. F. *Int. J. Mass Spectrom. Ion Processes* **1990**, *98*, 69–78.

(11) (a) Turecek, F.; Drinkwater, D. E.; McLafferty, F. W. *J. Am. Chem. Soc.* **1989**, *111*, 7696–7701. (b) Turecek, F.; McLafferty, F. W.; Smith, B. J.; Radom, L. *Int. J. Mass Spectrom. Ion Processes* **1990**, *101*, 283–300. (c) Egsgaard, H.; Carlsen, L.; Florencio, H.; Drewello, T.; Schwarz, H. *Chem. Phys. Lett.* **1988**, *148*, 537–540.

(12) (a) Sulzle, D.; Schwarz, H. *Chem. Phys. Lett.* **1989**, *156*, 397–400. (b) Polce, M. J.; Wesdemiotis, C. *Proceedings of the 39th ASMS Conference on Mass Spectrometry and Allied Topics*; Nashville, TN, 1991; p 1572.

(13) (a) Wesdemiotis, C.; Feng, R.; Williams, E. R.; McLafferty, F. W. *Org. Mass Spectrom.* **1986**, *21*, 689–695. (b) Lorquet, J. C.; Leyh-Nihant, B.; McLafferty, F. W. *Int. J. Mass Spectrom. Ion Porcesses* **1990**, *100*, 465–475.

(14) Turecek, F.; Gu, M.; Shaffer, S. A. *J. Am. Soc. Mass Spectrom.* **1992**, *3*, 493–501.

(15) Dawson, P. H. *Mass Spectrom. Rev.* **1986**, *5*, 1–37.

(16) Drinkwater, D. E.; Turecek, F.; McLafferty, F. W. *Org. Mass Spectrom.* **1991**, *26*, 559–562.

(17) Hehre, W. J.; Radom, L.; Schleyer, P. v. R.; Pople, J. A. *Ab Initio Molecular Orbital Theory*; Wiley: New York, 1986.

(18) Frisch, M. J.; Head-Gordon, M.; Schlegel, H. B.; Raghavachari, K.; Binkley, J. S.; Gonzalez, C.; DeFrees, D. J.; Fox, D. J.; Whiteside, R. A.; Seeger, R.; Melius, C. F.; Baker, J.; Martin, R. L.; Kahn, L. R.; Stewart, J. J. P.; Fluder, E. M.; Topiol, S.; Pople, J. A. *GAUSSIAN 88*; Gaussian Inc.: Pittsburgh, 1988.

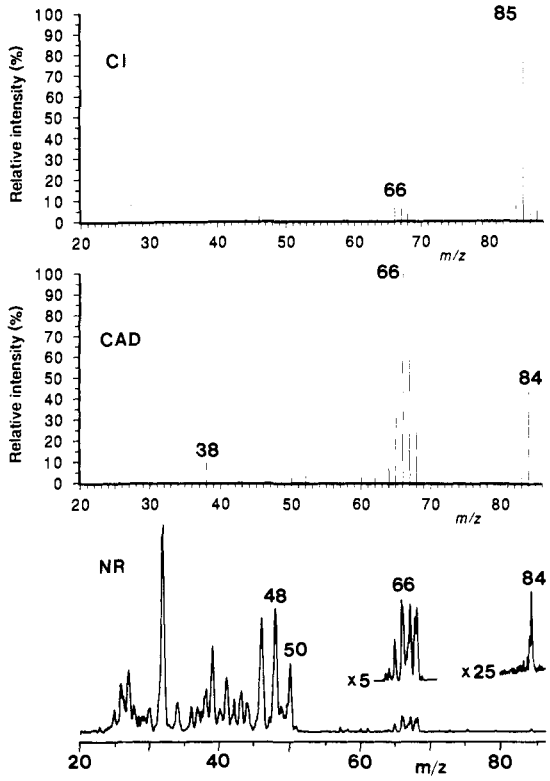

Figure 2. Top, isobutane chemical ionization mass spectrum of $(CD_3)_2SO$; middle, collisionally activated dissociation (O_2, 70% transmittance) mass spectrum of 2^+; bottom, neutralization–reionization (Xe/O_2, 70%/70% transmittance) mass spectrum of 2^+.

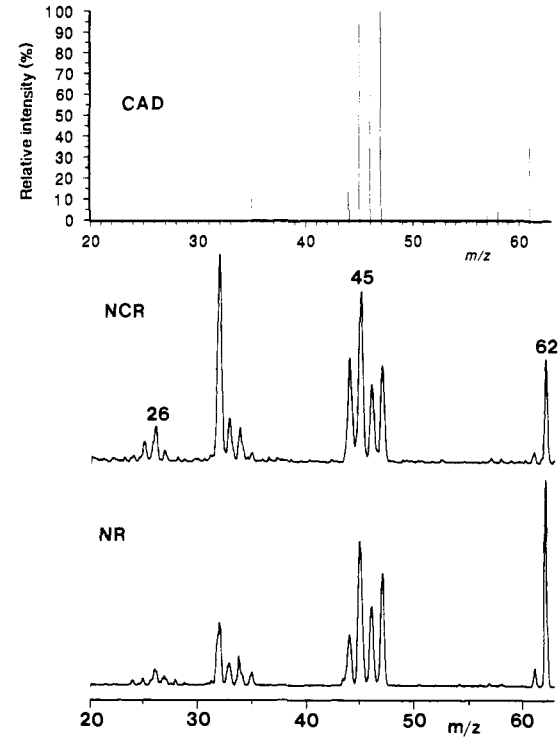

Figure 3. $(CH_3)_2S^{\bullet+}$: top, Collisionally activated dissociation mass spectrum (O_2, 70% transmittance); middle, neutralization–collisional activation–reionization ($Xe/He/O_2$, 70%/33%/70% transmittance) mass spectrum; bottom, neutralization–reionization (Xe/O_2, 70%/70% transmittance) mass spectrum.

calculate relative energies at 0 K as discussed in the text. In order to compare the calculated relative energies with the experimental data, the scaled harmonic frequencies were further used to calculate product enthalpies and relative energies at 298 K.

Results and Discussion

Gas-phase protonation of DMSO with $C_4H_9^+$ in isobutane plasma is a mildly exothermic process, $-\Delta H_r = 14$ kJ mol^{-1}, based on the corresponding proton affinities (PA(DMSO) = 834 kJ mol^{-1}, PA(i-C_4H_8) = 820 kJ mol^{-1}).[19] Accordingly, 1^+ undergo negligible (<10%) fragmentation. The dissociations observed are loss of methyl, methane, hydroxyl, and water to form $CH_3SOH^{\bullet+}$, CH_3SO^+, $(CH_3)_2S^{\bullet+}$, and $CH_3SCH_2^+$, respectively (Figure 1). The CAD spectrum of nondissociating 1^+ also shows dominant eliminations of methyl, methane, hydroxyl, and water (Figure 1). These fragmentations are consistent with structure 1^+ and suggest that ions 1^+ do not isomerize before reaching the collision region. Moreover, stable $(CH_3)_2S^+OH$ is known to exist as a hexachlorotellurate(IV) in both solution and the solid state as confirmed by X-ray structure analysis.[20]

The CI mass spectrum of 2^+ (Figure 2) shows a peak at m/z 66 due to elimination of CD_3H and/or HDO, while a peak at m/z 65 is missing, suggesting that no elimination of CD_4 takes place in these ion source dissociations. Elimination of CD_3H presumably leads to the formation of CD_3SO^+, which is a stable species.[11a] By contrast, the CAD spectrum of 2^+ does contain peaks at m/z 65 and 64 (Figure 2). The former, presumably $CD_2{=}SOH^+$,[11a] can be formed by elimination of CD_4 from 2^+ or by CAD of the intermediate $CD_3SOH^{\bullet+}$ (m/z 67), as reported previously.[11a]

In contrast to the stability of the protonated dimethylsulfoxide ion, no significant surviving precursor ions are found in the $^+NR^+$ mass spectra of 1^+ and 2^+ (Figures 1 and 2). The very weak peak at m/z 79 cannot be assigned unequivocally to surviving **1**, as it may be due to the reionized isotope satellites ($^{13}CCH_6OS$ and/or $C_2H_6O^{33}S$) of stable residual $(CH_3)_2SO^{\bullet+}$ (Figure 1). The absence of reionized $1^{\bullet+}$ and $2^{\bullet+}$ indicates that the intermediate radicals **1** and **2** are unstable on the time scale used in these measurements. From the time of flight of 8-keV **1** (4.5 μs) and the signal-to-noise ratio ($\approx$400) we estimate the maximum half-life of **1** as $\tau < 5 \times 10^{-7}$ s, corresponding to a unimolecular dissociation rate constant $k > 1.3 \times 10^6$ s^{-1}. This represents a lower limit in keeping with the previous estimates of $k = 3.5 \pm 2 \times 10^6$ s^{-1}.[3]

The $^+NR^+$ spectrum of 1^+ differs substantially from its CAD spectrum in both primary fragment formation and their further dissociations. Radical **1** dissociates by loss of methyl and hydroxyl to give rise to CH_3SOH and $(CH_3)_2S$, respectively, that are reionized to the corresponding ions of m/z 64 and 62. The loss of water, typical of 1^+ CAD, is insignificant in dissociations of neutral **1**. The primary products undergo further substantial dissociations. CH_3SOH dissociates to form $^{\bullet}CH_2SOH$ at m/z 63 by loss of H$^{\bullet}$, and $SOH^{\bullet}$ at m/z 49 by loss $CH_3^{\bullet}$. Subsequent dissociations produce CH_2SH, CH_2S, CHS, CS, and S. Fragmentation of the CH_3SOH formed from **1** is much more extensive than that of CH_3SOH formed upon neutralization with Xe or Hg of the stable $CH_3SOH^{\bullet+}$.[11a] Under the latter conditions CH_3SOH shows a predominant survivor ion (34% of the total reionized ion current), while the fragments are less abundant.[11a] However, the $^+NR^+$ spectrum of **1** shows a CH_3SO^+ fragment at m/z 63 which is typical of dissociation of the $CH_3SOH^{\bullet+}$ *ion*, while disfavored in the dissociation of collisionally activated *neutral* CH_3SOH.[11a] We explain the formation of $CH_3SO^{\bullet}$ by dissociations of $(CH_3)_2SO$ formed by hydrogen loss from **1** (see discussion below).

The increased fragmentation of CH_3SOH from **1** suggests that the dissociation of the latter is exothermic and large internal energy is imparted into the primary products. This was further examined with $(CH_3)_2S$, the other product of **1** dissociations. Neutral $(CH_3)_2S$ shows an abundant survivor ion upon neutralization–reionization (Figure 3). However, the fragment ion relative abundances in the $^+NR^+$ spectrum differ from those in the electron impact[21] and CAD mass spectra (Figure 3). Namely, the low

(19) Lias, S. G.; Liebman, J. F.; Levin, R. D. *J. Phys. Chem. Ref. Data* **1984**, *13*, 695–808.

(20) Viossat, B.; Khodadad, P.; Rodier, N. *J. Mol. Struct. (THEOCHEM)* **1981**, *71*, 237–244.

(21) McLafferty, F. W.; Stauffer, D. B. *The Wiley/NBS Registry of Mass Spectral Data*; Wiley-Interscience: New York, 1989; Vol. 1., p 6.

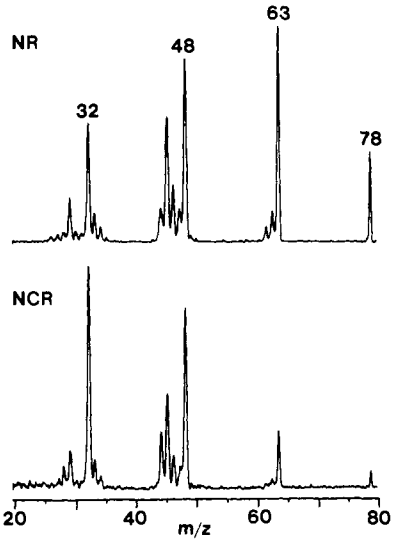

Figure 4. $(CH_3)_2SO^{\bullet+}$: top, Neutralization–reionization (Xe/O_2, 70%/70% transmittance) mass spectrum; bottom, neutralization–collisional activation–reionization ($Xe/He/O_2$, 70%/33%/70% transmittance) mass spectrum.

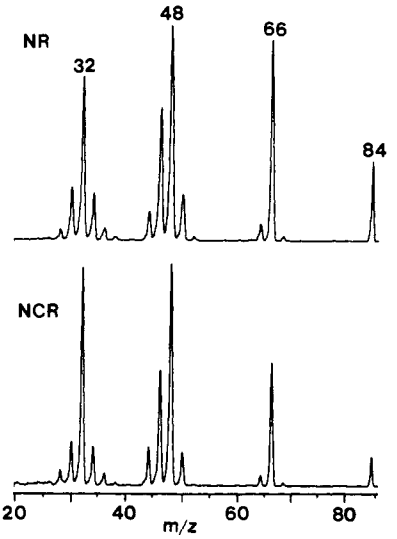

Figure 5. $(CD_3)_2SO^{\bullet+}$: top, Neutralization–reionization (Xe/O_2, 70%/70% transmittance) mass spectrum; bottom, neutralization–collisional activation–reionization ($Xe/He/O_2$, 70%/33%/70% transmittance) mass spectrum.

relative abundances of typical ion dissociation products such as H_3S^+ and $CH_3SCH_2^+$ (m/z 35 and 61, respectively, Figure 3) indicate that the $^+NR^+$ mass spectrum displays mostly products of neutral dissociations. The different behavior of $(CH_3)_2S$ and $(CH_3)_2S^{\bullet+}$ is compatible with their dissociation thermochemistries. Thus loss of H$^\bullet$ from $(CH_3)_2S$ is 390 kJ mol^{-1} endothermic, while the loss of methyl requires 323 kJ mol^{-1} and thus should be preferred.[22] The loss of H$^\bullet$ from $(CH_3)_2S^{\bullet+}$ requires ~217 kJ mol^{-1},[22] while the rearrangement to CH_2SH^+ and $CH_3^\bullet$ requires 223 kJ mol^{-1},[22] making these ion dissociations competitive.

The separation of neutral and ion dissociations in the $^+NR^+$ spectrum of $(CH_3)_2S$ is due in part to the experimental setup, as the time scale for the neutral dissociations is about 10 times longer than that for dissociations of ions following reionization.[14] Note that any ions formed by reionization with helium in the neutral drift region retain their kiloelectronvolt kinetic energy and are filtered out.[14] Likewise, <3% of the helium atoms used for neutral collisions can enter the cells and cause neutralization or reionization to promote ion dissociations. Neutral collisional activation with He enhances formation of stable neutral products, e.g., CHS, CS, and S. The latter fragment dominates the $^+NCR^+$ spectrum obtained at 33% transmittance (multiple collision conditions).[29] Note that the stepwise formation of S from $(CH_3)_2S$ is 606 kJ mol^{-1} endothermic,[23] suggesting substantial neutral excitation in these multiple collisions.[29d] Atomic sulfur and CHS are also the predominant fragments of neutral **1** dissociations under $^+NR^+$ conditions (Figure 1).

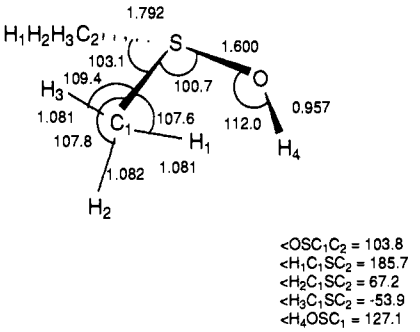

Figure 6. Optimized geometry of $\mathbf{1}^+$.

The $^+NR^+$ spectrum of $\mathbf{2}^+$ shows a weak peak of $(CD_3)_2SO^{\bullet+}$ at m/z 84 in addition to those of CD_3SOH (m/z 67), $(CD_3)_2S$ (m/z 68), and their dissociation products. The $^+NR^+$ spectrum of **2** further shows peaks at m/z 66 and 65. The former fragment cannot be due to D loss from $(CD_3)_2S$, which is a minor process under $^+NR^+$ conditions (vide supra). CD_3SOH was found to lose mostly D upon $^+NR^+$,[11a] which accounts for the formation of $^\bullet CD_2SOH$ at m/z 65. The fragment at m/z 66 is therefore mostly $CD_3SO^\bullet$ formed from $(CD_3)_2SO$. Both the ion $(CD_3)_2SO^{\bullet+}$ and the neutral $(CD_3)_2SO$ are expected to dissociate readily by CD_3 loss. For example, the formation of CH_3SO^+ from $(CH_3)_2SO^{\bullet+}$ requires 157 kJ mol^{-1} [30] and represents the major dissociation in the CAD spectrum of the latter ion.[31] The dissociation energy of the C–S bond in neutral $(CH_3)_2SO$ is estimated as 230 kJ mol^{-1}.[25] Dissociations of $(CH_3)_2SO$ and $(CD_3)_2SO$ in $^+NR^+$ and $^+NCR^+$ are shown in Figures 4 and 5. Both $(CH_3)_2SO^{\bullet+}$ and $(CD_3)_2SO^{\bullet+}$ show substantial survivor ions, while CH_3SO^+ and CD_3SO^+, respectively, are the major products in their dissociations. Neutral collisional activation leads to decrease of relative intensities of both reionized $(CH_3)_2SO^{\bullet+}$ and CH_3SO^+, while the $[CH_3SO^+]/[(CH_3)_2SO^{\bullet+}]$ abundance ratio increases from 2.3 in the $^+NR^+$ to 3.5 in the $^+NCR^+$ spectrum (Figure 4). The relative abundance of $(CD_3)_2SO^{\bullet+}$ in both the $^+NR^+$ and $^+NCR^+$ spectra (11% and 3%, respectively) is higher than that of $(CH_3)_2SO^{\bullet+}$ (9% and 2%, respectively), showing a small isotope effect. The more rapid dissociation of $(CH_3)_2SO$ may account for its absence in the $^+NR^+$ spectrum of **1**, while a small fraction of $(CD_3)_2SO$ from **2** survives and is detected after reionization. It should be noted that the $^+NR^+$ and $^+NCR^+$ spectra of $(CH_3)_2SO^{\bullet+}$ are

(22) From (kJ mol^{-1}) the C–H bond dissociation energy in CH_3XCH_3 (390) and the heats of formation of $(CH_3)_2S$ (−37.5),[23] H$^\bullet$ (218), CH_3 (146),[24] $CH_3S^\bullet$ (139–143),[25,26] $(CH_3)_2S^{\bullet+}$ (801),[24] CH_2SH^+ (862),[24] and $CH_3SCH_2^+$ (~800, corrected to 298 K).[24] The energy excess in the CH_2SH^+ formation is ca. 16 kJ mol^{-1}.[27,28]

(23) Pedley, J. B.; Rylance, J. *Sussex N.P.L. Computer Analyzed Thermochemical Data, Organic and Organometallic Compounds*, University of Sussex: Sussex, 1977.

(24) Lias, S. G.; Bartmess, J. E.; Liebman, J. F.; Holmes, J. L.; Levin, R. D.; Mallard, W. G. *J. Phys. Chem. Ref. Data, Suppl. 1* **1988**, *17*, 68–70.

(25) Benson, S. W. *Chem. Rev.* **1978**, *78*, 23–35.

(26) McMillen, D. F.; Golden, D. M. *Annu. Rev. Phys. Chem.* **1982**, *33*, 493–532.

(27) Butler, J. J.; Baer, T.; Evans, S. A. *J. Am. Chem. Soc.* **1983**, *105*, 3451.

(28) Radom, L.; Bouma, W. J.; Nobes, R. H.; Yates, B. F. *Pure Appl. Chem.* **1984**, *56*, 1831–1842.

(29) (a) Cooks, R. G., Ed. *Collision Spectroscopy*, Plenum: New York, 1978. (b) Kim, M. S. *Int. J. Mass Spectrom. Ion Processes* **1983**, *50*, 189–203. (c) Kim, M. S. *Int. J. Mass Spectrom. Ion Processes* **1983**, *51*, 279–290. (d) For a recent review, see: Kim, M. S. *Org. Mass Spectrom.* **1991**, *26*, 565–574.

(30) Zha, Q.; Nishimura, T.; Meisels, G. G. *Int. J. Mass Spectrom. Ion Processes* **1988**, *83*, 1–12.

(31) Carlsen, L.; Egsgaard, H. *J. Am. Chem. Soc.* **1988**, *110*, 6701–6705.

Table I. Total Electronic Energies

species	total energy[a] HF/6-31G*	MP2/6-31G*	MP4/6-31G*	ZPVE[b,c]	H_{298}[b,d]
$(CH_3)_2S^+OH$	-551.900 548	-552.462 448	-552.523 867	228	249
$(CH_3)_2S^•OH$	-552.006 479	-552.581 882	-552.641 910	228[e]	249[e]
$(CH_3)_2SO$	-551.537 278	-552.110 898	-552.170 217	203	220
$(CH_3)_2S$	-476.735 334	-477.120 666	-477.174 326	193	208
$CH_3SCH_2^•$	-476.108 141	-476.469 715	-476.522 547	156	172
CH_3SOH	-512.530 521	-512.964 156	-513.008 022	131	146
$CH_3S^•$	-437.101 471	-437.330 619	-437.367 247	92	103
CH_3OH	-115.035 418	-115.344 928	-115.372 340	131	142
H_2O	-76.010 747	-76.195 957	-76.206 318	54	64
$OH^•$	-75.382 275	-75.520 643	-75.535 617	21	27
$CH_3^•$	-39.558 991	-39.668 670	-39.689 177	73	84
$H^•$	-0.498 233				4

[a] In hartrees. $\langle S^2 \rangle$ in all UHF calculations were <0.76 after spin annihilation. [b] In kJ mol^{-1}. [c] From 6-31G* harmonic frequencies scaled by 0.9. [d] Includes ZPVE and 298 K vibrational, rotational, and translational contributions calculated within the rigid rotor–harmonic oscillator approximation. [e] Assumed to be the same as in 1^+.

substantially different from the ion collisionally-activated dissociation spectrum that shows significant loss of water by ionic rearrangement.[31]

In summarizing this part, **1** and **2** are found to undergo fast dissociations by simple cleavages of bonds in the vicinity of the hypervalent sulfur atom to form $(CH_3)_2SO$, CH_3SOH, and $(CH_3)_2S$ that further dissociate to ultimately form SO, CHS, CS, and S.

While **1** and **2** do not survive 4.5 μs after ion neutralization, their existence as equilibrium structures in very shallow potential energy minima cannot be excluded from the above experiments alone. In addition, unfavorable Franck–Condon factors in vertical neutralization can lead to fast dissociation of even relatively stable species.[32] Therefore, relative stabilities of **1** and its dissociation products have been assessed by ab initio calculations.[17,18] Geometry optimizations of **1** starting from the 6-31G* optimized geometry of ion 1^+ failed to find a local minimum. Upon attempted optimization structure **1** (Figure 6) collapses to $(CH_3)_2S$ and $OH^•$ with a large initial energy gradient along the S–O dissociation coordinate (226 kJ mol^{-1} Å^{-1}) that smoothly decreases with increasing S–O bond length. Similar results were obtained by starting the optimization at different S–O bond lengths (1.50, 1.55, and 1.70 Å). Optimizations with S–O bond lengths fixed at the above values led to collapse by S–C bond cleavage to give nonrelaxed CH_3SOH and $CH_3^•$. Both the absence of an equilibrium structure for **1** and the large calculated energy gradients indicate that the minimum does not exist or is extremely shallow. Unfortunately, the size of **1** precludes using an optimization method that would account for electron correlation effects. Nevertheless, we believe that a potential energy minimum of 54 kJ mol^{-1}, as suggested previously,[3] would have been found at the present level of theory.

The calculated electronic energies for 1^+, vertically formed **1**, and neutral dissociation products are summarized in Table I. Table II gives the corresponding relative energies at 0 and 298 K. The calculations indicate that **1** produced by vertical neutralization is a high-energy species that dissociates exothermically. The most exothermic dissociation channel is due to the formation of methanol and methylthiyl radical. However, this requires a rearrangement in **1** accompanied by hydroxyl group migration from the sulfur atom to one of the methyl groups. Since rearrangements usually have nonzero activation energies, the formation of $CH_3S^•$ and CH_3OH is not expected to compete with the direct cleavage dissociations despite its greater exothermicity. Accordingly, no detectable peak of reionized CD_3OH is found in the $^+NR^+$ spectrum of **2**, whereas the peaks of $CD_3S^•$ from **2**, and $CH_3S^•$ and CH_3OH from **1** would overlap with other fragments. Elimination of water from **1** is calculated to be another highly exothermic process (Table II) giving rise to the $CH_3SCH_2^•$ radical. Again, a unimolecular loss of water would require a tight four-membered transition state of a substantial activation energy.[33] The absence of a $CH_3SCH_2^•$ peak at m/z 61 in the $^+NR^+$ spectrum of **1** indicates that the elimination of water is not competitive in **1** dissociations.

Table II. Relative Energies in the C_2H_7OS System

species	E_{rel}[a,b]	$\Delta H_{r,298}$[a,c]	ΔH_f
$(CH_3)_2S^•OH$	0	0	
$(CH_3)_2SO + H^•$	-95	-98	67[d]
$CH_3SOH + CH_3^•$	-169	-164	-44[e]
$(CH_3)_2S + OH^•$	-193	-193	1.5[f]
$CH_3SCH_2^• + H_2O$	-246	-241	
$CH_3S^• + CH_3OH$	-261	-260	-58.5[g]

[a] In kJ mol^{-1}. [b] MP4/6-31G* + ZPVE relative energies, 0 K. [c] Including 298 K heat contents. [d] From $\Delta H_f(H^•)$ = 218 kJ mol^{-1} [24] and $\Delta H_f(CH_3SOCH_3)$ = -151.3 kJ mol^{-1}.[23] [e] From $\Delta H_f(CH_3SOH)$ = -190 kJ mol^{-1} [34] and $\Delta H_f(CH_3^•)$ = 146 kJ mol^{-1}.[24] [f] From $\Delta H_f(CH_3SCH_3)$ = -37.5 kJ mol^{-1} [23] and $\Delta H_f(OH^•)$ = 39 kJ mol^{-1}.[24] [g] From $\Delta H_f(CH_3S^•)$ = 143 kJ mol^{-1} [25] and $\Delta H_f(CH_3OH)$ = -201.6 kJ mol^{-1}.[23]

The direct bond cleavage dissociations show widely varying exothermicities (Table II). Note that all the values refer to **1** configuration as formed by vertical neutralization of 1^+, and not to a relaxed structure. The cleavage of the S–O bond in **1** is calculated to be the most favored dissociation, consistent with the large energy gradient in **1** along the S–O coordinate. From the point of view of the dimethyl sulfide and hydroxyl radical reactants, the reaction is expected to have a substantial activation barrier. Although we have not sought the transition state of the dimethylsulfide–hydroxyl reaction directly, incremental calculations (UHF/6-31G*) at different C–S and S–O bond lengths point to a saddle point >150 kJ mol^{-1} above the reactants.

Dissociation of **1** to CH_3SOH and $CH_3^•$ is calculated to be 29 kJ mol^{-1} less exothermic than that leading to $(CH_3)_2S$ and $OH^•$. This contradicts predictions from the experimental heats of formation that should prefer the former route by ca. 42 kJ mol^{-1}.[23,34] This discrepancy may be due to some uncertainty in the heat of formation of CH_3SOH. For example, the present calculations (Table I, MP4/6-31G* + ZPVE + H_{298} corrections)) predict the dissociation $CH_3SOH \rightarrow CH_3S^• + OH^•$ to be endothermic by 262 kJ mol^{-1} at 298 K, indicating $\Delta H_f(CH_3SOH)$ = -80 kJ mol^{-1}. This differs significantly from both the experimental and MNDO-calculated values (-190 and -155 kJ mol^{-1}, respectively).[34]

The loss of the hydroxyl hydrogen atom from **1** is calculated to be 90 kJ mol^{-1} (65 kJ mol^{-1} from the experimental heats of formation, Table II) less exothermic than the cleavage of the S–O bond. The simultaneous occurrence of these diverse dissociations, as observed in the $^+NR^+$ spectrum of **2**, is remarkable, since rate constants differing by several orders of magnitude should be expected. Similar effects have been observed earlier for disso-

(32) Hop, C. E. C. A.; Holmes, J. L. *Int. J. Mass Spectrom. Ion Processes* **1991**, *104*, 213–226.

(33) Maccoll, A. *Chem. Rev.* **1969**, *69*, 33–60.

(34) Turecek, F.; Brabec, L.; Vondrak, T.; Hanus, V.; Hajicek, J.; Havlas, Z. *Collect. Czech. Chem. Commun.* **1988**, *53*, 2140–2158.

ciations of hypervalent radicals produced by neutralization of stable ions.[7] Although we have no rigorous explanation of this phenomenon, it appears that **1** is initially formed in a variety of excited electronic states due to the very fast electron transfer and the virtually random orientation of the ion and neutral counterparts. An unbound electronic state of the neutral will dissociate rapidly on the particular potential energy surface that may be different from that calculated for **1** that leads to the S-O bond rupture. In this model, the branching ratio will depend on the initial electronic state population rather than the dissociation kinetics.

Conclusions

Dimethylhydroxysulfuranyl radical **1** does not survive 4.5 μs after having been formed by vertical neutralization of the dimethylhydroxysulfonium ion, and dissociates exothermically by cleavages of the C-S, O-S, and O-H bonds. No stable equilibrium structure is found for **1** by ab initio calculations that also predict exothermic dissociation. **1** thus represents a transition state rather than an intermediate in the atmospherically important oxidation of dimethyl sulfide with hydroxyl radicals.

Acknowledgment. We gratefully acknowledge the generous financial support by the National Science Foundation (Grant CHEM-9102442), the University of Washington Graduate School Fund, the donors of the Petroleum Research Fund, administered by the American Chemical Society, for partial supports of this work, and the computational support by the Cornell National Supercomputer Facility which receives major funding from the National Science Foundation and the IBM corporation, with additional support from the New York State and the Corporate Research Institute.

Supplementary Material Available: Listing of 6-31G* and 3-21G calculated harmonic vibrational frequencies of sulfur-containing species (1 page). Ordering information is given on any current masthead page.

Formation of $LaCoO_3$ Highly Dispersed on ZrO_2

Noritaka Mizuno,*,† Hiroaki Fujii,‡ Hiroshi Igarashi, and Makoto Misono*

Contribution from the Department of Synthetic Chemistry, Faculty of Engineering, The University of Tokyo, Hongo, Bunkyo-ku, Tokyo 113, Japan. *Received February 5, 1992*

Abstract: The well-characterized La-Co oxide overlayer was prepared on the surface of ZrO_2 powder by impregnating ZrO_2 with aqueous solutions of the mixtures of La and Co acetates followed by calcination at various temperatures. The preparation processes and the structure of La-Co oxide overlayers were investigated in detail by IR, XRD, XPS, EDX, TEM, and adsorption of NO and pyridine. It was concluded that a highly dispersed La-Co oxide overlayer which may have the $LaCoO_3$ perovskite structure was formed. The resulting La-Co/ZrO_2 catalysts showed very high catalytic activities for complete oxidation of propane.

Introduction

Metal oxide overlayers on the surface of metal oxides or metals have attracted much attention in the fields of materials science, electrochemistry, corrosion, heterogeneous catalysis, and so on, owing to their specific surface reactivity and electrical or tribological properties. So, the investigation of the process of growth of the oxide overlayer is interesting for the better understanding and precise control of the surface reactivity and electrical or tribological properties.

Perovskite-type mixed oxides, ABO_3 (A = La, Ca, Sr, Ba, etc.; B = Co, Ti, Mn, etc.), have important physical properties such as ferro-, piezo-, and pyroelectricity, magnetism, electrooptic effects, and superconductivity. In addition, perovskites are good catalysts for various reactions: oxidation of CO and hydrocarbons, reduction of NO and SO_2, hydrogenation and hydrogenolysis of hydrocarbons, etc.[1-3] Perovskites containing Co or Mn show high catalytic activity for the complete oxidation of CO, CH_4, and C_3H_8;[4-10] e.g., the catalytic activity of $La_{0.8}Sr_{0.2}CoO_3$ is comparative to or higher than that of Pt catalysts and $La_{0.9}Ce_{0.1}CoO_3$ was actually used as a commercial catalyst.[11]

Although the perovskite catalysts are thermally more stable and less expensive than noble metal catalysts, the surface area is low. If the perovskites were directly supported on high surface area supports, they would be much more attractive catalysts in practice. However, the solid-state reactions between perovskite components and the support oxides to form other stable mixed oxides often take place. For example, Co-containing perovskites cannot be directly supported on alumina-based oxides, since cobalt atoms are incorporated into the bulk of the support to form a spinel ($CoAl_2O_4$),[6,7] so that the majority of cobalt atoms cannot contribute to the catalytic activity.

In earlier works, perovskite particles were supported on cordierite and alumina by using aqueous slurries containing powdered perovskite, cordierite or alumina, and stearic acid.[8,9] But the reaction between the perovskite particle and support to form less reactive mixed oxides was not avoidable. Recently, several new methods have been attempted,[10,12-18] such as precoating of the

* Author to whom correspondence should be addressed.
† Present address: Catalysis Research Center, Hokkaido University, Sapporo 060, Japan.
‡ Present address: Kuraray Co., Ltd., Kaigan-dori, Okayama 702, Japan.

(1) Voorhoeve, R. J. H. In *Advanced Materials in Catalysis*; Burton, J. J., Garten, R. L., Eds.; Academic Press: New York, 1977; pp 129-180.
(2) Tejuca, L. G.; Fierro, J. L. G.; Tascon, J. M. D. in *Advances in Catalysis*; Eley, D. E., Pines, H., Weisz, P. B., Eds.; Academic Press: San Diego, 1989; Vol. 36, p 237. Misono, M., Lombardo, E. A., Eds. Perovskite. *Catal. Today* **1990**, *8*, 133-275.
(3) Mizuno, N. *Catal. Today* **1990**, *8*, 221-230.
(4) Nakamura, T.; Misono, M.; Uchijima, T.; Yoneda, Y. *Nippon Kagaka Kaishi* **1980**, 1679-1684.
(5) Nakamura, T.; Misono, M.; Yoneda, Y. *J. Catal.* **1983**, *83*, 151-159.
(6) Arnoldy, P.; Moulijn, J. A. *J. Catal.* **1985**, *93*, 38-54.
(7) Massoth, F. E. In *Advances in Catalysis*; Eley, D. E., Pines, H., Weisz, P. B., Eds.; Academic Press: New York, 1978; Vol. 27, pp 265-310.
(8) Gallagher, P. K.; Johnson, D. W., Jr.; Schrey, F. *Mat. Res. Bull.* **1974**, *9*, 1345-1352.
(9) Chien, M. W.; Pearson, I. M.; Nobe, K. *Ind. Eng. Chem. Prod. Res. Dev.* **1975**, *14*, 131-134.
(10) Nudel, J. N.; Umansky, B. S.; Lombardo, E. A. *Appl. Catal.* **1987**, *31*, 275-289.
(11) Tabata, K.; Misono, M. *Catal. Today* **1990**, *8*, 249-261.
(12) Fujii, H.; Mizuno, N.; Misono, M. *Chem. Lett.* **1987**, 2147-2150.

0002-7863/92/1514-7151$03.00/0